

S-Gears Made of Polymers

Gorazd HLEBANJA, Simon KULOVEC, Jože HLEBANJA, Jože DUHOVNIK

Abstract: Metals are the prevailing material in gear manufacturing, whereas new materials based on various polymers are gaining in importance due to their characteristics, e.g. mass properties, ease of manufacturing, damping ratio, lower noise, etc. Involute gears are perfected to a high level in today gear industry. At the same time, involute gears have some weak points. S-gear tooth flank and S-gear tooth geometry were developed in this context. Therefore, the purpose of this paper is to present the essential properties of S-gears and how they can be used not only on a macro scale (e.g. in wind power plants) but also on a micro scale in small mechanisms using polymers as their basic material. A special testing rig was developed at FME Ljubljana and thus some preliminary testing issues are discussed in the paper.

Keywords: polymer gears; involute gears; S-gears; S-gear properties; polymer gear testing

1 Introduction

We owe the basic principles of contemporary gearings to Charles-Étienne Louis Camus [1] and to Leonhard Euler [2] who established these independently. Euler also sought the involute shape of gear teeth flanks [3] which is in common use today. He also showed how to graphically determine the radii of curvature. Cycloids, involutes and rolling curves can be used to form gear teeth according to the law of gearing.

Gradual development enabled the evolution of the optimal shape of the involute gears which transmit power by the convex-convex contact. The curvature radius function of the involute gear is growing constantly over the involute. This also implies that the curvature radii values in the dedendum part

when approaching the base circle are small and limit to zero at the base circle and therefore imply high contact loads in this area, *Fig. 1*. Additionally, for gears with a low number of teeth the dedendum flank is comparatively short and thus leading to excessive sliding and friction losses. Yet another problem is the undercutting of the dedendum area. This was why many researchers and engineers sought new solutions, and the concave-convex gear pair appears to be an obvious solution. This is the intrinsic feature of the S-gear shape, which is discussed later in this paper.

2 S-gear geometry

A basic requirement when defining gear tooth flank geometry is that a

rack tooth flank as well as a driving and a driven gear flank imply the same path of contact and that they follow the law of gearing. Several mathematical curves meet these requirements, e.g. cycloids, involutes and similar curve families. These principles are valid even in the cases where one of the above elements is defined whereas the others, depending on it, derive from there. This gives the designer some freedom to adapt to the particular features which gears should inherit [5]. Starting with these considerations, the rack tooth flank profile of the proposed gears is defined by the following expression [6]:

$$y_{pi} = a_p (1 - (1 - x_{pi})^n) \quad (1)$$

where (x_{pi}, y_{pi}) are Cartesian coordinates originating in the pitch point C, the a_p parameter designates the

Dr. Gorazd Hlebanja, univ. dipl. inž., Higher Education Centre, School of Technologies and Systems, Novo Mesto, Slovenia; dr. Simon Kulovec, univ. dipl. inž., Podkrižnik, d. o. o., Ljubno ob Savinji, Slovenia; Prof. em. dr. Jože Hlebanja, univ. dipl. inž., prof. dr. Jože Duhovnik, univ. dipl. inž., both University of Ljubljana, Faculty of Mechanical Engineering, Ljubljana, Slovenia

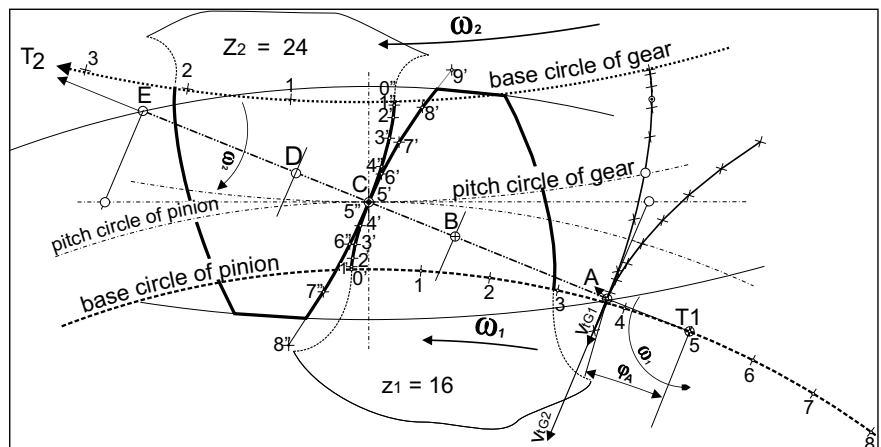


Figure 1. Circumstances at the meshing start in involute gears [4]

size factor ($a_p = 1.30267$), and n is the exponent ($n = 1.9$). Both, a_p and n , have a decisive influence on the expected characteristics of the designed gears. The rack profile is thus defined by the analytical function for which the derivatives exist as well. Eq. (1) defines the addendum part of the rack profile and the half symmetric counterpart defines its dedendum part.

Knowing $y' = f'(x)$ one can calculate the path of contact simply by $y_{U_i} = y_{P_i}$ and $x_{U_i} = y_{P_i} y_{P_i}'$. This means that for any basic rack profile there exists only one path of contact. Nevertheless, arbitrary numbered gears derive from there. The lowest possible number of teeth can be as low as four, whereas a rack can be treated as a gear with an infinite number of teeth.

The rolling principle – the rack’s datum line rolls over the kinematic circle of the gear – is employed to define the gear tooth flank. So, any point of the gear flank G_i is cut in the contact point U_i on the path of contact. The gear tooth flank is rotated so that the tangent of G_i corresponds to the tangent of the rack point P_i in the contact point U_i . If the rack and gear flank are pushed to the coordinate system origin in C , the rack is translated back for the distance $U_i P_i$. The angle of rotation is defined by an arc based on the kinematic circle of the gear of the same size.

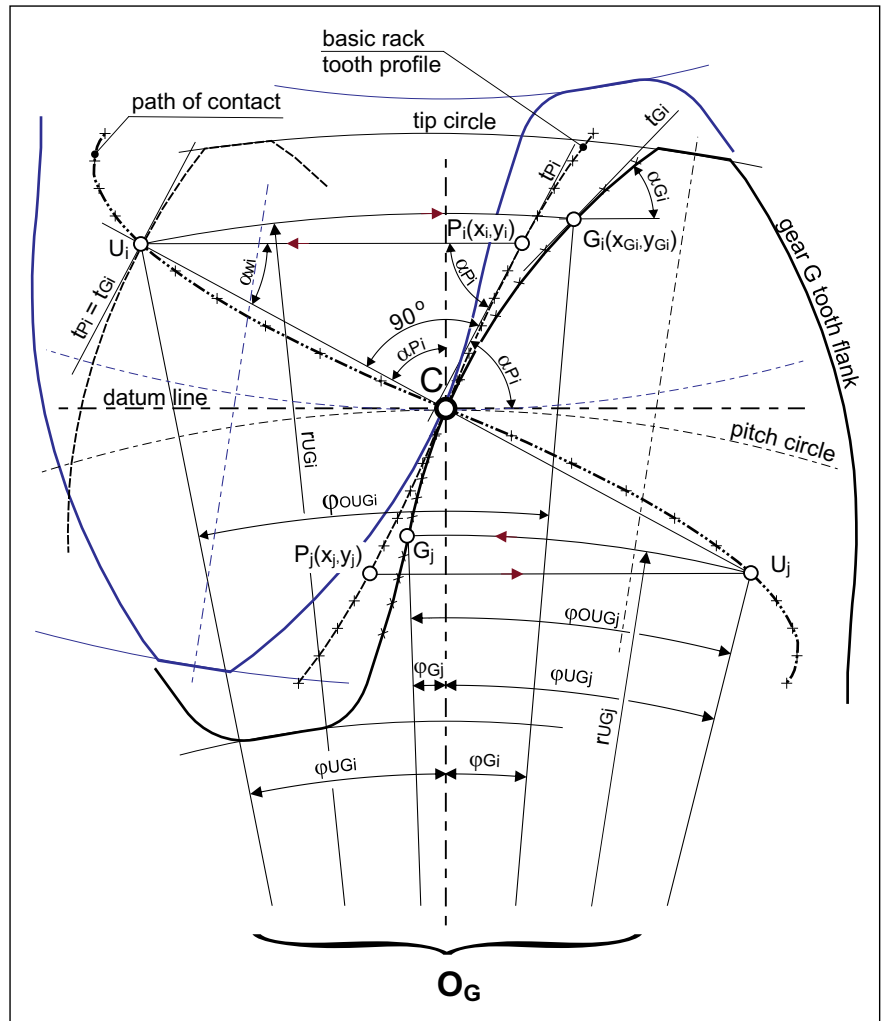


Figure 2. S-gear tooth flank profile creation

procedure transforming an arbitrary point P_i (on the rack) to U_i (on the path of contact) and furthermore to G_i (pinion) and H_i (gear) defines unique points and that the inverse transformation copies back to the deriving point.

■ 3 Important features

3.1 Curvature radii and flank pressure

The curvature radii of the gear flanks can be computed simply by

$$\varphi_{OU} = (x_U + x_P) / r_0 \quad (2)$$

The radius r_U and φ_U of U_i on the path of contact are calculated through x_{U_i} , y_{U_i} and r_0 . Based on this we get:

$$\varphi_G = \varphi_{OU} - \varphi_U \quad (3)$$

and the Cartesian coordinates of G_i are

$$\begin{aligned} x_G &= r_U \sin \varphi_G \\ y_G &= r_U \cos \varphi_G - r_0 \end{aligned} \quad (4)$$

The mating gear can be defined similarly. We can conclude that the

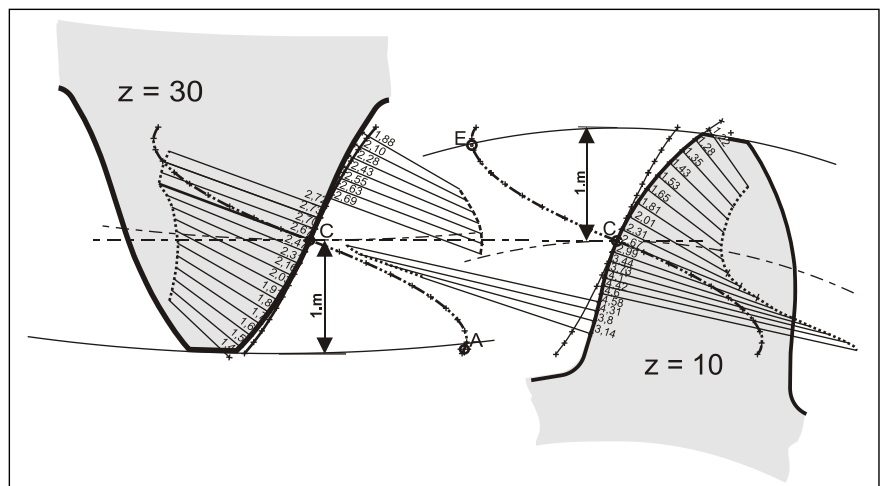


Figure 3. Radii of curvature along the driving and the driven gear tooth flank

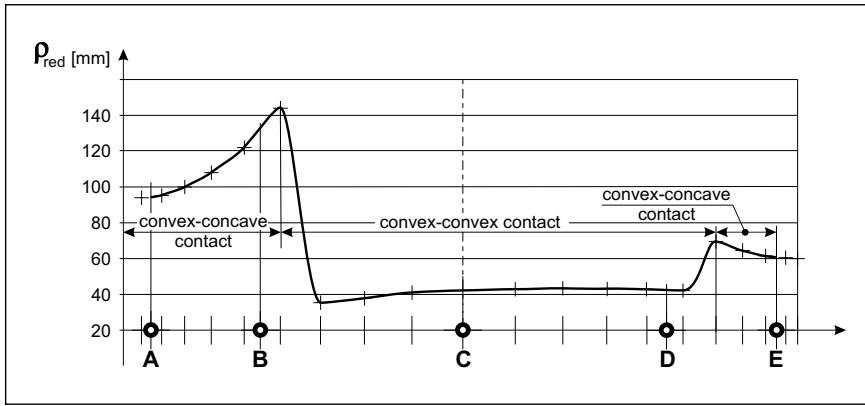


Figure 4. Reduced radii of the curvature for $z_1 = 10$, $z_2 = 30$ and $m = 30$ mm

the defining equation for the curvature, i.e.

$$\frac{1}{\rho} = \lim_{\Delta s \rightarrow 0} \frac{\Delta \alpha}{\Delta s} \quad (5)$$

where $\Delta \alpha$ stands for the change of the direction angle and Δs for the increase of length of a curve. Unlike with the involute gears, the change of direction of the curvature can be observed in S-gears, Fig. 3. Namely, the flank shape becomes concave in the dedendum part of a gear. The concave part is rather small for a low number of teeth and extends near the pitch circle for a bigger number of teeth [6], [7], [8].

This assures a convex-concave contact in the vicinity of the meshing start and meshing end, since the dedendum of one gear meshes with the addendum of the other. Therefore, the contact circumstances in this critical area are improved. However, with regard to the contact pressure, the reduced radii of curvature have to be computed (Eq. 6). The distribution of the reduced radii is diagrammatically represented in Fig. 4.

$$\rho_{red} = \frac{\rho_1 \rho_2}{\rho_1 \pm \rho_2} \quad (6)$$

The distribution of the reduced radii of the curvature over the path of contact, Fig. 4, reveals some interesting facts. First, there are comparatively high values of ρ_{red} in the zones AB and DE, which are due to a convex-concave contact, indicating that the contact load is smaller and lubrication conditions are better. Second, two pairs of teeth are in contact in AB and DE. Both maximums are due

to the change of direction when the flank curve switches from concave to convex. ρ_{red} is relatively constant and has its maximum in the pitch point in the zone of the single pair contact BCD, which indicates an evenly distributed power transmission. The actual curve depends on geometrical data, i.e. the number of teeth of both gears and the module.

The dedendum part of a tooth flank is the most loaded area in power transmission from a gear to a pinion due to the negative sliding in that area. This is why this loading

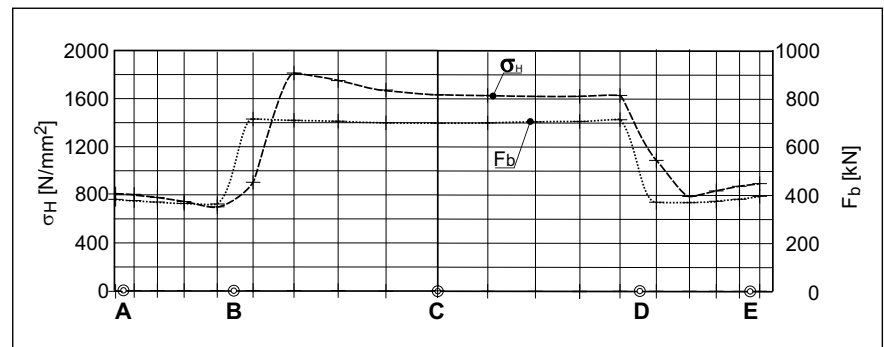


Figure 5. Hertzian pressure and contact force along the path of contact; actual data $m = 30$ mm; $b \approx 6.7 m = 200$ mm; $E = 2.06 \times 10^6$ N/mm²; $\nu = 0.3$

state is of a particular importance. The contact load at a particular contact point in time appears in the contact spot on the path of contact and is influenced by the contact force F_b which is acting rectangular to the teeth flanks in the direction of the kinematic pole C. The contact force magnitude along the path of contact is variable, conforming to the changes of the pressure angle α_w along the path of contact (Eq. 7). Hertzian pressure is a common measure of the contact load of the

mating teeth flanks, Eq. 8. Hertzian pressure may not exceed the maximal allowable limit σ_{Hdop} . The contact force F_b , the tooth width b and the reduced radii of the curvature ρ_{red} and material properties are those design parameters which decisively influence gear durability, where only ρ_{red} deals with the tooth flank geometry. The tangential force F_t , transmitted from the driving to the driven gear, is distributed among two gear pairs in the zones of double contact AB and DE. This is also true for F_b , which can be observed in Fig. 5.

$$F_b = \frac{F_t}{\cos \alpha_w} \quad (7)$$

$$\sigma_H = \sqrt{\frac{F_b E}{2\pi b \rho_{red} (1 - \nu^2)}} \leq \sigma_{Hdop} \quad (8)$$

3.2 Velocity circumstances

Velocity circumstances in the gear tooth contact, appearing along the path of contact, decisively influence the oil film thickness and depend on the tooth flank geometry. Absolute

velocities, relative velocities of the teeth flanks, and the contact point movement velocity in the tangential direction to the path of contact can be distinguished with regard to the tangential direction to the teeth flanks in the contact point. Two critical states are illustrated in Fig. 6: that is, the critical state in the vicinity of the meshing start and the one in the vicinity of the meshing end area. The absolute velocity of the pinion tooth flank is represented by vector \mathbf{v}_g and the absolute velocity of the

gear by \mathbf{v}_p . The relative velocities \mathbf{v}_{rS} and \mathbf{v}_{rP} act tangentially to the corresponding tooth flanks, whereas \mathbf{v}_{At} is the velocity of the contact point in the direction of the tangent to the path of contact. Thus, the expressions for \mathbf{v}_s and \mathbf{v}_p are

$$\vec{v}_S = \vec{\omega}_S \times \vec{r}_S \text{ and } \vec{v}_P = \vec{\omega}_P \times \vec{r}_P \quad (8)$$

The velocity components in the direction of the teeth flank surfaces influence the oil film formation; for the corresponding velocities of the pinion, \mathbf{v}_{rS} and the gear \mathbf{v}_{rP} are

$$\vec{v}_{rS} = \vec{v}_S - \vec{v}_{At} \text{ and } \vec{v}_{rP} = \vec{v}_P - \vec{v}_{At} \quad (9)$$

The sliding velocity \mathbf{v}_g is defined as the difference between the absolute velocities of teeth flanks in the contact point or as the difference between relative velocities.

$$\vec{v}_g = \vec{v}_S - \vec{v}_P = \vec{v}_{rS} - \vec{v}_{rP} \quad (10)$$

3.3 Oil film thickness

The prevailing belief among experts is that the cause of micro-pitting damages, particularly on slow running gears, is mixed lubrication [9, p. 311]. Since insufficient oil film formation does not ensure total surface separation, the asperities of the meshing teeth surfaces come to metal contact. The oil film thickness is influenced by: load, contacting teeth flank surfaces velocities in actual contact, sliding velocities, temperature, surface roughness, oil characteristics, material properties, and tooth shape, actually transmit

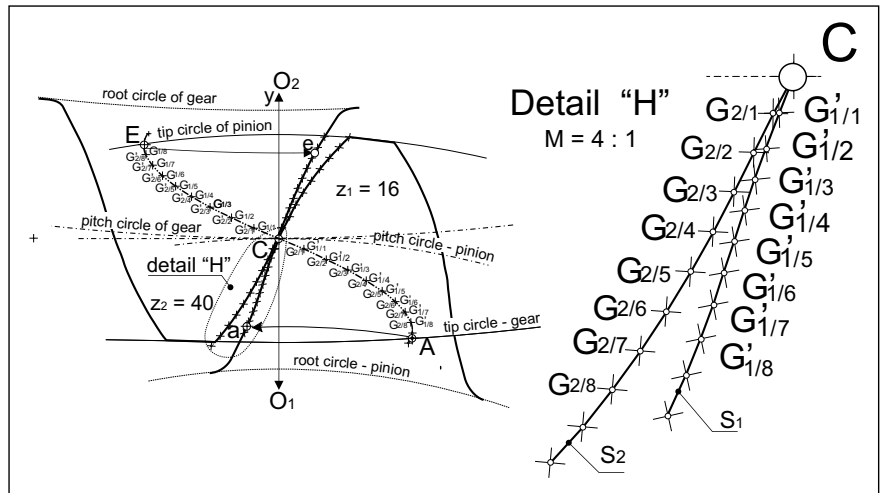


Figure 7. Contact density [4]

load. The dimensioning of gears when taking into consideration the micro-pitting is based on oil film thickness based on the elasto-hydrodynamic lubrication theory. The original research of the EHL was conducted by Dawson and Higginson who also developed the empirical equation for EHL film thickness [10]. The following equation [9] was used for a general elliptic type of contact in order to get the basic relations:

$$\frac{h_0}{R'} = 3,63 \left(\frac{u \eta_0}{E' R'} \right)^{0,68} (\alpha E')^{0,49} \left(\frac{W}{E' R'^2} \right)^{-0,073} (1 - 0,61e^{-0,68k}) \quad (11)$$

where h_0 stands for the minimal oil film thickness [m]; R' is the reduced curvature radius in the contact point [m]; u is the average of the contact velocities [m/s]; E' is the reduced elasticity module [Pa]; α is the pressure viscosity coefficient

[m²/N]; η_0 is the dynamic viscosity at atmospheric circumstances [Pa s]; W is the load [N]; $k = a/b$ is the ellipticity parameter where a and b stand for ellipse axes. In the case of cylindrical contact surfaces, k limits to ∞ and the exponential part of Eq. 11 limits to 0. The former equation can finally be rearranged to

$$h_0 = [3,63 \eta_0^{0,68} \alpha^{0,49} E'^{-0,117}] u^{0,68} \rho^{0,466} W^{-0,073} \quad (12)$$

The value of the product in the square brackets is a constant for a particular case, provided that the temperature is kept constant, whereas the tangential velocities (Fig. 6), the reduced radii of the curvature (Fig. 4) and the load vary along the path of contact. The prevailing factors conserving the oil film thickness are the dynamic viscosity (oil property) and the sum of relative velocities which are higher in the vicinities of meshing start and meshing end points due to the curved path of contact.

3.4 The rolling-sliding ratio

Fig. 7 illustrates the contact density of the driving dedendum, designated by G_{2i} , and driven addendum, designated by G_{1i} . One can observe that the dedendum part is shorter, which depends on the number of teeth – the lesser the number of teeth the shorter the length of the dedendum. Accordingly, the addendum part is longer, which in-

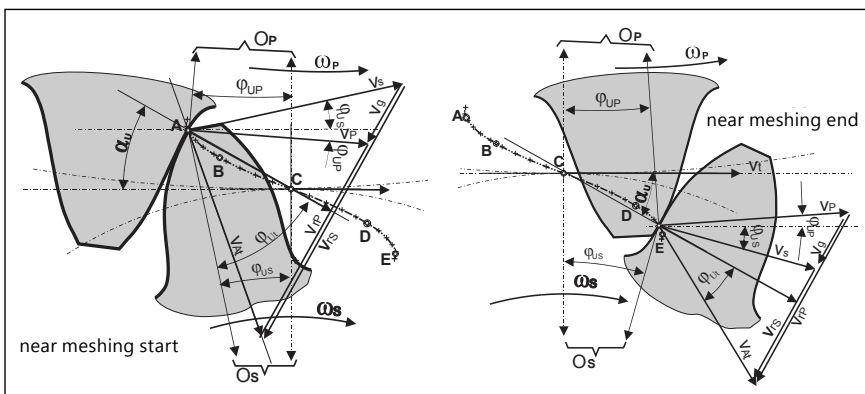


Figure 6. Velocity circumstances for S-gears in the meshing start area (above) and in the meshing end area (below) [8]

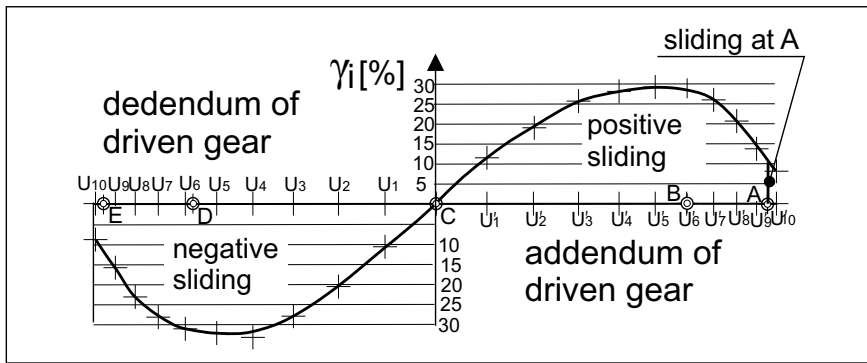


Figure 8. Specific sliding

indicates that the driving dedendum contact point density is higher than in the driven gear addendum.

If both densities were equal, pure rolling would have resulted. The density difference therefore indicates the amount of sliding of the partner with the longer intermediary path that is the path with lesser density. So, if we designate the path on the dedendum partner with s_{1i} and the path on the addendum flank with s_{2i} , we can write formally

$$\Delta s_i = s_{2i} - s_{1i} \tag{13}$$

The smaller of the two, s_{1i} or s_{2i} gives the value for pure rolling and the difference, Δs_i , gives the value of sliding. Of course, the situation is reversed for the upper side, above C.

Specific sliding is defined as a quotient $\gamma_i = \Delta s_i / s_{1i}$, meaning the slide-to-roll ratio in an arbitrary contact point U_i . Fig. 8 illustrates the situation. The sliding of one flank on the other always means lost energy. An important attribute of the S-gears is that more power is transmitted from the driving to the driven gear by rolling and less by sliding, which is a comparative advantage. It is particularly important that a greater part of energy is transmitted by rolling also in the vicinity of the meshing start point, A.

■ 4 Variation of parameters

Eq. 1 reveals that only two parameters rule the flank shape, namely the exponent n and the form (height)

factor a_p , which define the rack profile and subsequent gear flank shape through a unique transformation. The third one, the inclination angle and the subsequent initial pressure angle depend on the former. In this way, root thickness can be increased, convex-concave zones can be tuned, and the initial pressure angle can be lowered (or increased).

Fig. 9 (a) shows the rack profile with $a_p = 1.303$, $n = 1.9$ and the inclina-

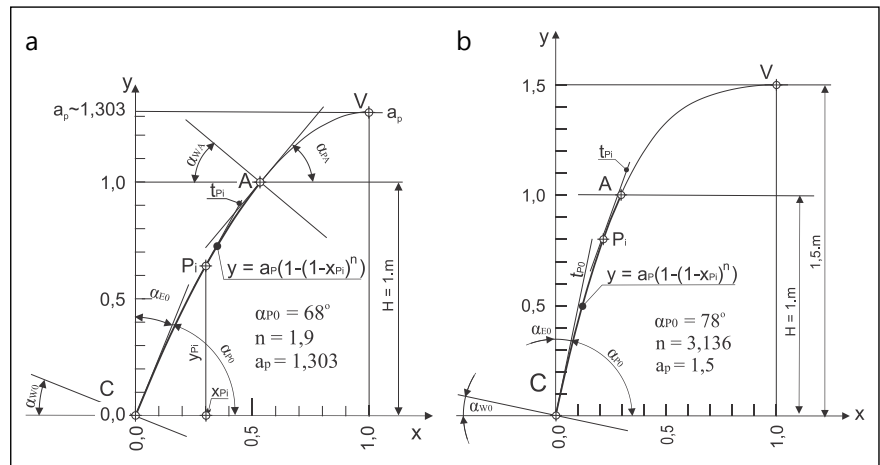


Figure 9. Basic rack tooth profile for inclination angles (a) 68° and (b) 78° [11]

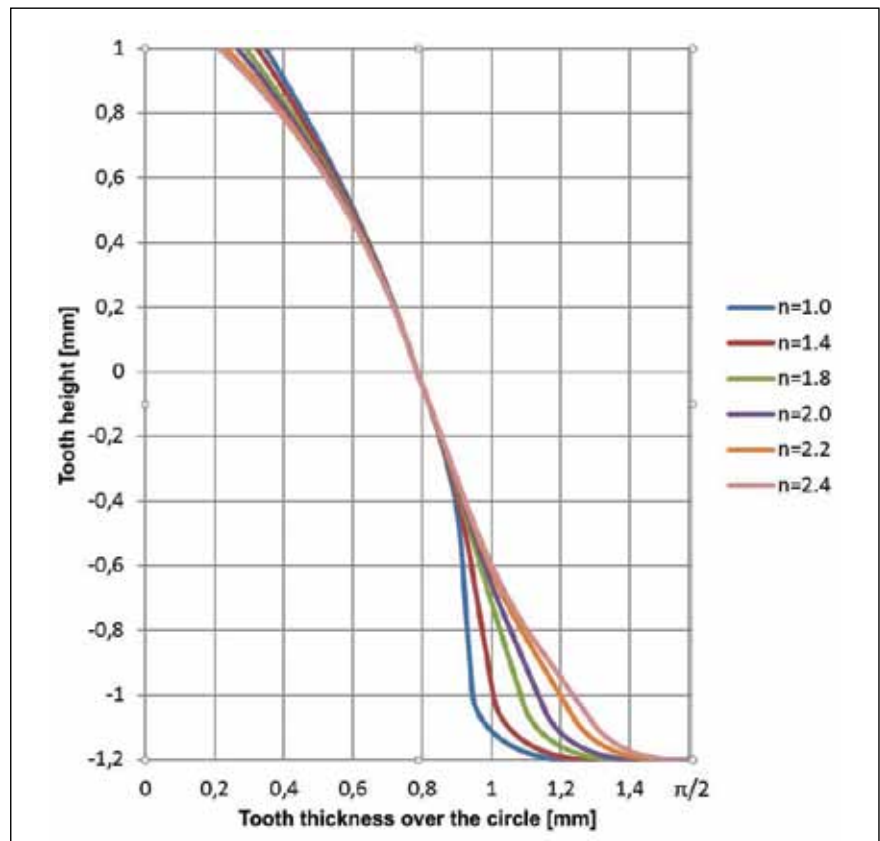


Figure 10. Tooth profile for pressure angle 20° vs. exponent n . The ordinate 0.00 represents the gear pitch circle; $m = 1 \text{ mm}$, $z_1 = 20$ [12]

tion angle $\alpha_{p0} = 68^\circ$. These parameters correspond to the pressure angle 22° . Accordingly, Fig. 9 (b) illustrates the rack profile with $a_p = 1.5$, $n = 3.136$ and the inclination angle $\alpha_{p0} = 78^\circ$. Both are compared in Fig. 9, which clearly reveals the essential differences between them [11].

The pressure angle is of a particular importance since it influences the flank load, the load capacity, and the curvature radii. There is common agreement that the pressure angle α_{w0} amounting to 22° is an optimum for the involute gears. This is also the reason for the selection of the same initial pressure angle for the S-gear rack, whereas the pressure angle elsewhere corresponds to the path of contact.

The parameters should be optimised in such a way that the produced gears conform to the anticipated requirements. S_{68} gears are strong in the root, whereas lowering the inclination angle even further gives even stronger root but at the same time the higher initial pressure angle induces a bigger contact force. The characteristics of the S_{78} gears are opposite to those of the S_{68} gears. The roots are thinner and the tips thicker. On the other hand, the contact force is lower and the contact ratio is essentially higher, as it can be observed in Fig. 11.

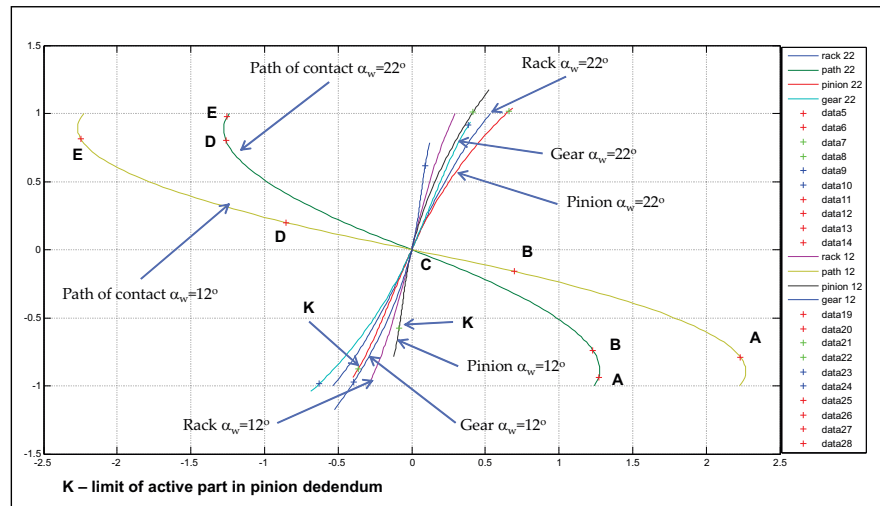


Figure 11. Effects of variation of the initial pressure angle

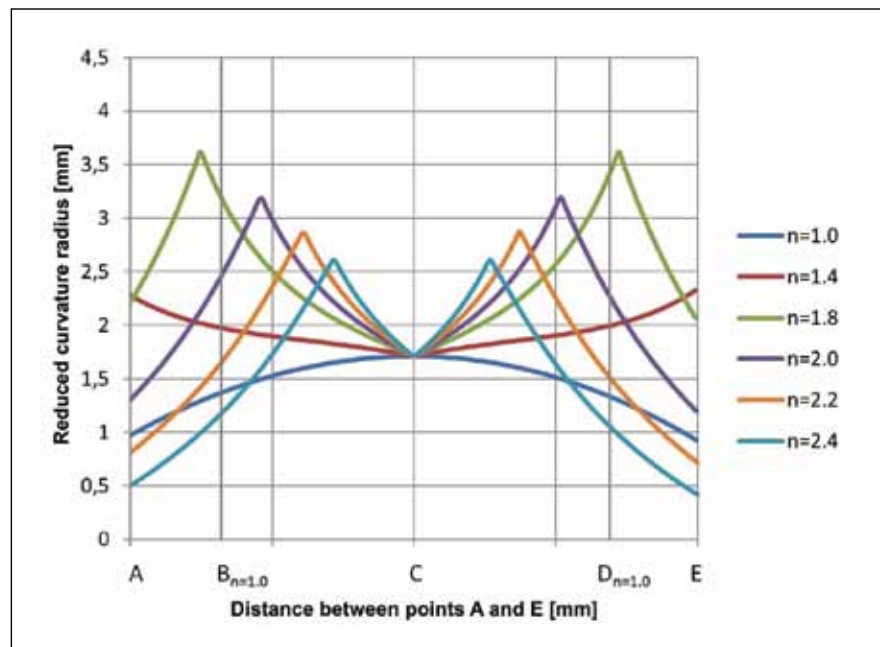


Figure 12. Dependence of the reduced radii of the curvature along the path of contact on the exponent n ; $\alpha_{w0} = 20^\circ$ $m = 1$ mm, $z_1 = z_2 = 20$ [12]

The lowering of the form factor a_p increases the curvature. The role of the exponent n is illustrated in Fig. 10. It can be seen that lower values of n induce a thinner root which becomes thicker for higher values of the exponent. On the other hand, higher values also induce a sharper tooth tip [12].

Teeth with a very strong root might be necessary for gears with a large load capacity, e.g. gears made of viscoelastic, polymeric or composite materials which exhibit less deformation and consequently less internal friction in dynamic applications.

The curvature radii and deriving reduced radii of the curvature are of the utmost importance due to their role

in the contact pressure where bigger radii imply lower contact pressure. Fig. 12 shows how the reduced curvature radii along the path of contact depend on the exponent n .

The maximums in the diagram are due to the change from concave to convex in a particular flank, and in this case, both sides are symmetric since both wheels have the same number of teeth. The increase of n also leads to a longer concave part. However, we are limited with the path of contact which should be pronouncedly curved and the active part should not reverse. With these limitations kept in mind, one

can conclude that the limiting exponent for the prescribed pressure angle is approximately 2.0 and the contact ratio 1.1219. If the exponent value is decreased, the path of contact becomes less curved and the contact ratio increases. So, a careful consideration of design data is necessary to define proper parameters in each individual case.

5 Gears made of polymers

S-gears have been initially developed for heavy duty applications in order to prevent scuffing and pitting

damages which had been developed with involute gears. Further development sought applications, e.g. gear-boxes of wind power plants, etc. Some advantages revealed in previous paragraphs, e.g. convex-concave contacts in the vicinities of the meshing start and meshing end points, the rolling-sliding ratio – that is, less sliding in the case of S-gears, etc., propose their use also in small scale and gear-boxes made of polymers and composite materials.

Despite several deficiencies, such as lower transmitted load, lower accuracy of moulded gears, dimensional problems (due to thermal expansion), temperature sensitivity, moulding tool cost and even possible chemical reactions, plastic gears are becoming more and more popular. This can be attributed to their qualities, such as low maintenance, wear resistance even when running dry, low noise, dampening of vibrations, noncorrosiveness, low inertia – low rotating mass, light weight, and low manufacturing cost. Every day, new and improved materials are invented which improve the known behaviour of gears made of various plastic materials.

Due to their advantages, the importance of materials like polymers is increasing rapidly. Excellent lifetime behaviour of such artefacts, e.g. gear trains, is expected.

Another important observation regarding gears is that even new guidelines, e.g. VDI 2736, Blatt 2 [13], are based on rather old experiments. Hachmann and Strickle have proposed their Eq. (14) for contact temperature already in 1966 [14].

$$T_{z1z2} = T_U + f_{ED} P \mu 136 \frac{i+1}{z_1 + 5i} \left(\frac{17100k_2}{b z_{1,2} (v m)^{3/4}} + 7,33 \frac{k_3}{A} \right) \quad (14)$$

This equation introduces parameters like ambient temperature (T_U), intermittence factor (f_{ED}), friction coefficient (μ), power (P), number of teeth (z), transmission ratio (i), tooth width (b), circumferential speed (v), module (m), surface of the gear box (A), material combi-



Figure 13. Experimental apparatus

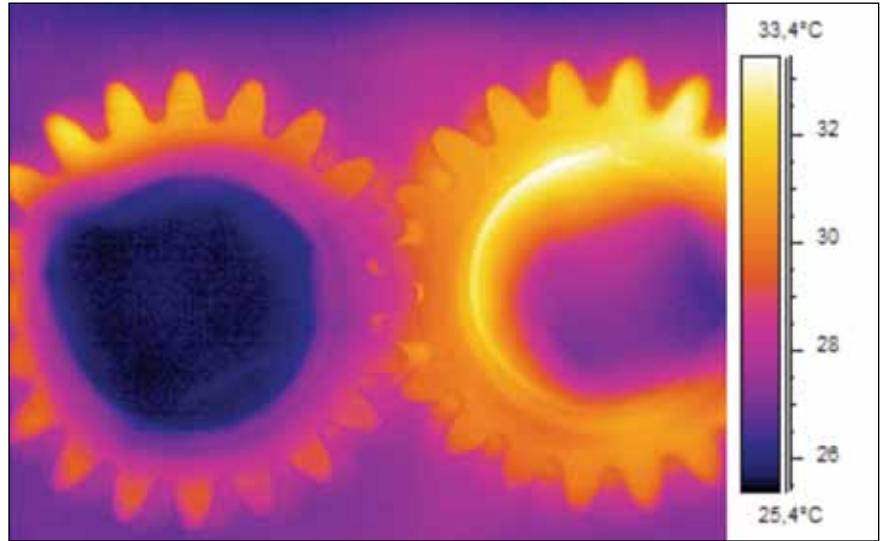


Figure 14. Picture made by a thermal camera

nation factor (k_2), gear case factor (k_3). This equation can only be valid for involute gears. Therefore, more testing is necessary to improve their work. As this equation cannot deal with S-gears, more testing is necessary in this context as well.

A special testing system has been built in order to test small plastic gears, with the module having around 1 and gears having around 20 teeth, Fig 13. Since the temperature behaviour of polymer gears in operation is important, the testing system was designed to enable observation of both gears in action by a fast thermal camera to reveal a temperature layout for a particular instant of the test, Fig. 14. The apparatus consists of two shortcut asynchronous motors powered by frequency inverters which enable a precise set up of speeds and subsequent amount of sliding. An adapting system allows an exact set up of the axis distance. Tests are meant to deliver Wöhler curves for each particular

material and geometry combination. Regarding materials, the POM – PA6 combination is mostly used due to better frictional behaviour.

Additionally, Fig. 15 reveals the initially manufactured S-gears ($\alpha_{v0} = 27^\circ$, $n = 1.4$) vs. the involute gears of the same size ($m = 1 \text{ mm}$, $z_1 = z_2 = 20$). The difference is obvious, but it can also be observed that the axis distance in the case of S-gears does not correspond to that of the involute gears. It is already agreed that S-gears can mate even with a disrupted axis distance [11], but the efficiency of the gears mating in this way has not been defined precisely, yet. This implies that the design of moulds should be carried out with the consideration of the actual shrinkage of particular materials in mind, which is not an easy task. Another consideration is that the quality of moulded gears is rather low, therefore it needs to be determined how it influences the precise flank geometry, particularly

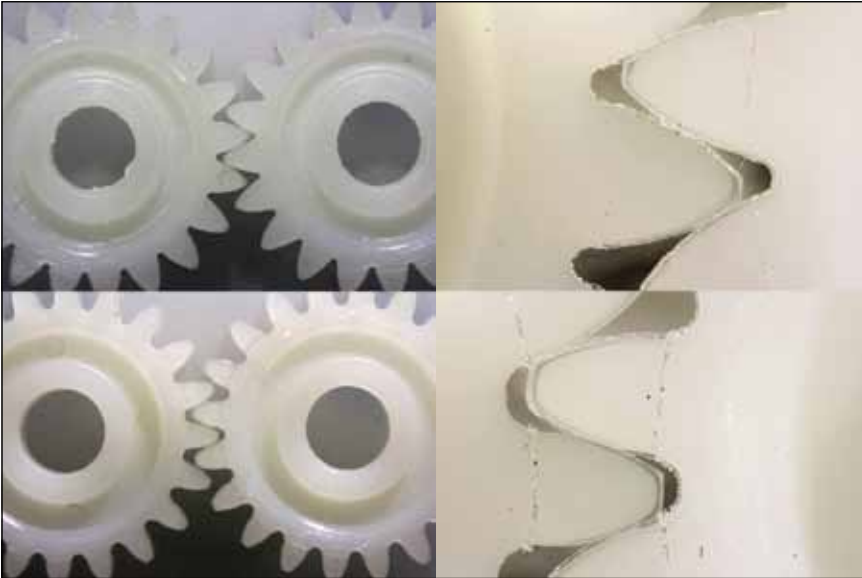


Figure 15. Comparison of S- (above) and E- gears (below)



Figure 16. Coordinate measuring machine (CMM) Wenzel Gear Tec

in the case of S-gears. Therefore, a lot of work has to be accomplished in order to gain useful results.

The shrinkage is inherent in the injection moulding process. Despite the fact that there are databases available for various materials and process parameters, it is difficult to propose correct values for a particular product and situation, e.g. injection moulded gears.

This is why a coordinate measuring machine (CMM) for gears should be used to measure the produced gears

and compare them to the theoretical shape. Deviations make the necessary corrections of the mould possible and in this way they enable a better accuracy of the final product. Such a CMM is LH54 Gear (Wenzel GearTec) with 4th axis rotary table, designed for measuring all types of gears (gear, shaft, worms, etc.) according to different standards for gear teeth quality. This machine with Metrosoft CM software is also used for the measurements of basic geometric elements and free form surfaces (based on a CAD model). With a scanning 3D probe, a large number

of measured points can be achieved. The machine has an active damping system and a good thermal stability through the use of dark granite for the base and axes air bearings to meet special requirements of high precision measurements.

■ 6 Conclusions

The solutions for preventing or diminishing micro-pitting occurrences are in general searched for in the direction of better lubrication means, high quality surface treatment (super-finishing), the gear tooth flank profile change in the meshing start area, and finally, better materials.

The S-gear tooth flank profile features a concave shape in the lower part of the dedendum. The mating gears exhibit convex-concave contact in the vicinity of the contact start and contact end. The S-gear tooth flank shape also assures higher comparative curvature radii. Therefore, the contact load is lower. The relative velocities in the contact surface are higher due to the curved path of contact, which implies better lubrication. Due to their S-shape, the velocity characteristics of mating gears are improved, especially in both external areas with high relative velocities and comparatively low sliding velocity.

The meshing start zone in involute gears represents a potential danger of micro-pitting, whereas S-gears exhibit an advantage in this context due to the thick oil film in this area which diminishes the possibility of damage. The high relative velocities of the mating flanks and the convex-concave contact in the vicinity of the meshing start point are decisive influencing factors.

Another important feature of the S-gears is a more evenly distributed contact point density which implies less sliding and lower power losses. The dedendum flank of the pinion is not substantially smaller than that of the gear addendum even for a low number of teeth.

It has also been proven that S-gears can mate even with changes in the axis distance [11]: that is, they are not sensitive in the context of cycloidal gears. However, the true impact of the axis distance variation in the context of efficiency still has to be assessed.

Authors believe that S-gears can be a useful replacement for the involute gears in many applications, both in large scale, e.g. wind power plants, and small scale, e.g. plastic gear-boxes for domestic appliances.

With regard to the definition of S-gears, by a parabolic type function defined rack profile defines a single path of contact and consequently gears with an arbitrary number of teeth. The defining parameters should be carefully chosen in order to assure design requirements. In this way, one could design gears with increased root thickness, gears with a low initial pressure angle, etc.

With regard to S-gears made of POM – PA6 and other polymeric and composite materials, one can conclude that the experimental work is in its initial phase. The testing system is operating, the testing procedure is established, however, there are two considerations that need to be elaborated. The first is the definition of the optimal form factor and the exponent in order to optimise the prescribed requirements. The second is the rather low quality of moulded gears which jeopardizes a correct assessment of the results. A helpful tool in this context is a 3D coordinate measurement machine with a rotary table, enabling gear tooth flank measurements.

References

- [1] Complete Dictionary of Scientific Biography (2008). "Camus, Charles-Étienne-Louis," from Encyclopedia.com: <http://www.encyclopedia.com/doc/1G2-2830900770.html> retrieved 14.8.2014.
- [2] The Euler Archive, s.v. "E249 -- De aptissima figura rotarum dentibus tribuenda," <http://eulerarchive.maa.org/pages/E249.html>, retrieved 22.8.2014.
- [3] Euler, L. (1760). *Novi Commentarii academiae scientiarum Petropolitanae* 5, 1760, pp. 299-316.
- [4] Hlebanja, G. (2012) S-gears for wind power turbine operating conditions. *Machine design*, ISSN 1821-1259, 2012, Vol. 4, No. 3, pp. 123-130.
- [5] Hlebanja, G. (2012) Characteristics of non-involute gears. In: Antunović, R. (Ed.). *Proceedings*. East Sarajevo, University of East Sarajevo, Faculty of Mechanical Engineering, 2012, pp. 9-20.
- [6] Hlebanja, J., Hlebanja, G. (2010) Spur gears with a curved path of contact for small gearing dimensions. *International Conference on Gears, Garching near Munich, Germany, Oct. 4-6, 2010: Europe invites the world, (VDI-Berichte, 2108)*. Düsseldorf: VDI-Verlag, 2010, pp. 1281-1294.
- [7] Hlebanja, G. (2011) Specially shaped spur gears: a step towards use in miniature mechatronic applications. *Balkan Journal of Mechanical Transmissions*, ISSN 2069-5497, 2011, Vol. 1, Iss. 2, pp. 25-31.
- [8] Hlebanja, G., Hlebanja, J. (2013) Contribution to the development of cylindrical gears. In: Dobre, G. (Ed.), Vladu, M. R. (Ed.). *Power transmissions: proceedings of the 4th international conference, Sinaia, Romania, June 20-23, 2012, (Mechanisms and machine science, ISSN 2211-0984, ISSN 2211-0992, Vol. 13)*. Dordrecht [etc.]: Springer, cop. 2013, pp. 309-320.
- [9] Stachowiak, G.W., (2006) Batchelor, A.W. *Engineering tribology*. Elsevier Butterworth-Heinemann.
- [10] Dowson, D., Higginson, G.R. (1977). *Elasto-Hydrodynamic Lubrication*. Pergamon Press.
- [11] Hlebanja, G., Hlebanja, J. (2013) Influence of axis distance variation on rotation transmission in S-gears: example on heavy duty gears. In: *International Conference on Gears, October 7th to 9th, 2013, Garching (near Munich), Germany: Europe invites the world, (VDI-Berichte, ISSN 0083-5560, 2199)*. Düsseldorf: VDI-Verlag, pp. 669-679.
- [12] Kulovec, S., Duhovnik, J. (2013) Variation of S-gear shape and the influence of the main parameters. In: *International Conference on Gears, October 7th to 9th, 2013, Garching (near Munich), Germany: Europe invites the world, (VDI-Berichte, ISSN 0083-5560, 2199)*. Düsseldorf: VDI-Verlag, cop. 2013, pp. 1535-1541.
- [13] VDI 2736, Blatt 2 (2013) Thermoplastische Zahnräder, Stirnradgetriebe, Tragfähigkeitsberechnung, VDI-Richtlinien, VDI, Düsseldorf.
- [14] Hachmann, H.; Strickle, E.; Polyamide als Zahnradwerkstoffe, 126, *Konstruktion*. 18 (1966) 3 pp. 81-94.

S-zobniki iz polimerov

Razširjeni povzetek

Kovine so prevladujoči material v proizvodnji zobnikov. Vsekakor pa novi materiali na podlagi različnih polimerov pridobivajo na pomenu zaradi svojih dobrih značilnosti, kot so masne lastnosti – majhni vztrajnostni momenti in masa, enostavna proizvodnja, zmožnost dušenja, manjša hrupnost, obrabne lastnosti itd., čeprav so dovoljene obremenitve manjše in je delovna temperatura omejena. Prav tako je izziv proizvodna kvaliteta in dimenzijska zanesljivost.

Evolventni zobniki, Eulerjev izum, ki v današnjem strojništvu prevladujejo skoraj v celoti, so bili v dolgi zgodovini deležni številnih izboljšav, tako da so v današnji industriji optimirani skoraj do popolnosti. Hkrati pa imajo evolventni zobniki nekaj šibkih točk. Tako zaradi narave evolvente postajajo radiji ukrivljenosti korena boka zoba vse manjši in limitirajo k nič, ko se približujemo osnovnemu krogu. To pa pogojuje večje bočne obremenitve v tem delu. Če ima pastorek hkrati še majhno število zob, je koren zoba zelo kratek, kar implicira čezmerno drsenje in torne izgube. Zato so raziskave, ki bi v celoti konveksno-konveksni stik evolventnih zobnikov nadomestile s konveksno-konkavnim stikom, ki bi pomenil bistveno manjše kontaktne obremenitve, pomembne. V teh okoliščinah se je razvilo S-ozobje z geometrijo bokov zob, pri kateri je stik na začetku vprijemne poti in na njenem koncu konveksno-konkaven, v osrednjem delu pa konveksno-konveksen. V pričujočem prispevku so predstavljene bistvene lastnosti S-ozobja, tj. radiji ukrivljenosti in bočni tlaki, hitrostne razmere zlasti na začetku ubiranja in na njegovem koncu, debelina oljnega filma in delež drsenja in kotaljenja. Prav to je pri S-ozobjih pomembno, ker sta vrh in koren zoba primerljive velikosti, kar pomeni bistveno manj drsenja in izgub.

S-zobniki so definirani z matematično enačbo boka zoba zobnice, ki ima dva parametra. Zobnica z določenim modulom definira eno samo ubirnico, ki pa definira stično krivuljo za zobnike s poljubnim številom zob. Variacije prej omenjenih parametrov bistveno vplivajo na lastnosti zobnika. Tako lahko ustvarimo zobe z zelo debelim korenem, ali pa take z majhnim vpadnim kotom.

Avtorji menijo, da lahko ozobja te vrste uporabljamo tako v makro aplikacijah, npr. planetni prenosniki vetrnih elektrarn, kot tudi v mikro aplikacijah, kot so manjši mehanizmi za avtomobilsko industrijo ali gospodinjske naprave, kjer pa so polimeri osnovni material. Na Fakulteti za strojništvo, v Centru za konstruiranje, so razvili posebno preizkuševališče za male zobnike iz polimerov. Preizkuševališče so preliminarno že uporabili za testiranje evolventnih zobnikov in S-zobnikov. Za zdaj uporabljena materiala sta bila za en zobnik POM in za drugi PA6. Hkrati pa ugotavljamo, da sta kvaliteta in dimenzijska zanesljivost plastičnih zobnikov bistveni. Skenirni 3D koordinatni merilni stroj z rotacijsko mizo in možnostjo meritev prostih ploskev je v tem okviru dragocen pripomoček, s katerim bomo pomembno izboljšali kvaliteto brizganih plastičnih zobnikov.

Ključne besede: zobniki iz polimerov, evolventni zobniki; S-zobniki; značilnosti S-zobnikov; testiranje zobnikov iz polimerov



ZASTOPA IN PRODAJA

ppt commerce d.o.o.

Celovška 334

1210 Ljubljana-Šentvid

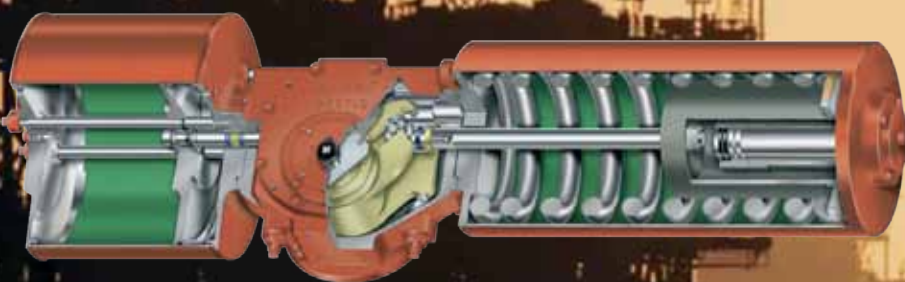
Slovenija

tel.: +386 1 514 23 54

faks: +386 1 514 23 55

e-pošta: ppt_commerce@siol.net

<http://www.ppt-commerce.si>



BETTIS™ pnevmatski in elektro aktuatorji